Electronic Supplementary Material (ESI) for ChemComm.

Assessing dimerisation degree and cooperativity in a biomimetic small-molecule model by pulsed EPR

K. Ackermann, A. Giannoulis, D. B. Cordes, A. M. Z. Slawin and B. E. Bode*

EaStCHEM School of Chemistry, Biomedical Sciences Research Complex and Centre of Magnetic Resonance, University of St Andrews, North Haugh, St Andrews KY16 9ST, UK.
E-mail: beb2@st-andrews.ac.uk

Supporting Information

Table of contents

1. General experimental information

Moisture- and air-sensitive reactions were performed under an atmosphere of nitrogen with the use of dry solvents, with glass-ware flame dried and cooled under nitrogen. Dry solvents (MeOH, DMF) were purchased from Sigma-Aldrich and were used as supplied. The solvent used for Sonogashira couplings (NEt_3) was freshly distilled from CaH_2, while all other solvents were used without further purification. Solvents used for Sonogashira coupling were degassed by freeze-pump-thaw cycles (× 3). Petrol refers to petroleum ether (boiling point 40-60 °C).

Room temperature (rt) refers to 20-25 °C. A temperature of 0 °C was achieved using an ice-water bath. Reflux conditions were achieved using the appropriate DrySyn heating block. The term *in vacuo* refers to the use of rotary evaporator.

Column chromatography was carried out either with silica gel 60 (Crawford Scientific) or with alumina, activated with 4% H_2O. Analytical thin layer chromatography was performed using pre-coated polystyrene TLC sheets or alumina TLC cards (Sigma-Aldrich). TLC visualization was carried out under ultraviolet lamp, followed by staining in 1% aq. $KMnO_4$ or 6% aq. vanillin.

Yields were calculated as amount of product [mmol] divided by the amount of the limiting reagent [mmol] and are given in %.

Melting points were recorded on an Electrothermal 9100 melting point apparatus and are uncorrected.

Infrared spectra were acquired on a Shimadzu Fourier transform IR Affinity-1 Infrared spectrometer.

NMR spectra were acquired on 300 MHz, Bruker Avance, 400 MHz, Bruker Avance, or 500 MHz, Bruker Ascend spectrometers in the deuterated solvent stated. Chemical shifts are quoted in parts per million (ppm) and referenced to the residual solvent peak(s). The abbreviations s, d, m denote singlet, doublet and multiplet respectively. Coupling constants (*J*) are reported in Hz.

Mass spectrometric (*m*/*z*) data were acquired by atmospheric pressure chemical ionisation (APCI), nanospray ionisation (NSI) and Matrix Assisted Laser Desorption/Ionisation (MALDI) at the EPSRC National Facility for Mass Spectrometry, Swansea.

2. Synthesis and characterisation of compound 1

(4'-iodo-[1,1'-biphenyl]-4-yl-1-oxyl-2,2,5,5-tetramethyl-2,5-dihydro-1*H*-pyrrole-3-carboxylate)

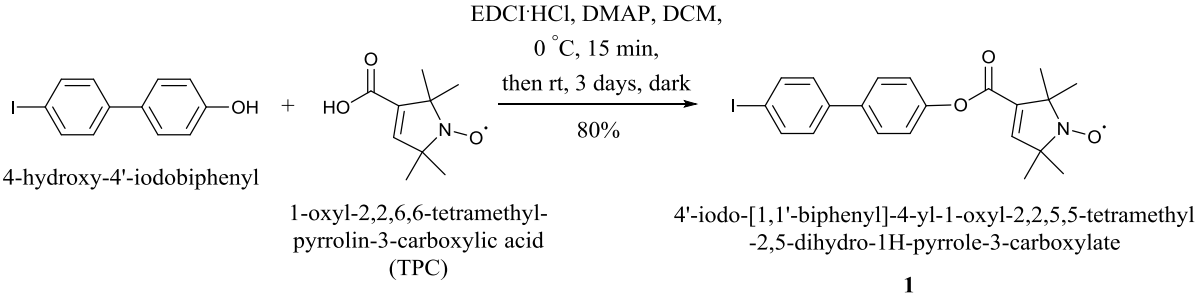

Scheme S1: Synthesis of compound **1**.

4'-iodo-[1,1'-biphenyl]-4-yl-1-oxyl-2,2,5,5-tetramethyl-2,5-dihydro-1*H*-pyrrole-3-carboxylate was prepared as described[1] with minor modifications. 1-oxyl-2,2,5,5-tetramethyl-pyrrolin-3-carboxylic acid (TPC) (0.30 g, 1.63 mmol) was dissolved in CH_2Cl_2 (15 mL) and the solution was left stirring at 0 °C for 10 min. 4-hydroxy-4'-iodobiphenyl (0.53 g, 1.8 mmol), DMAP (0.02 g, 0.16 mmol) and EDCI·HCl (0.33 g, 1.72 mmol) were added and the reaction mixture was left stirring at 0 °C for 5 min and then at rt for 3 days in the dark. The solvent was removed *in vacuo*, the crude product was redissolved in CH_2Cl_2 (20 mL), washed with sat. $NaHCO_3$ (2 × 20 mL) and dist. H_2O (2 × 20 mL) and dried over Na_2SO_4. The layers were separated and removal of the solvent *in vacuo* yielded the crude product, which was purified by column chromatography on alumina (2.5 × 16 cm, 4% H_2O) using petrol/EtOAc (8/2) as eluent to give the title compound (0.58 g, 1.27 mmol, 80%) as an intense yellow powder. Single crystals suitable for X-ray were obtained by recrystallisation from chloroform.

Formula: $C_{21}H_{21}INO_3$.

ν_{max}/cm^{-1} 754s, 802s, 999s, 1026s, 1168s, 1201s, 1730 (C=O), 2796s.

δ_H(500 MHz; CD_2Cl_2) 1.29 (1 H, s, 6C*H*$_3$), 7.25 (2 H, s, Ar*H*), 7.37 (2 H, d, Ar*H*), 7.64 (2 H, s, Ar*H*), 7.81 (2 H, d, Ar*H*).

The ^{1}H NMR of the reduced (by phenylhydrazine) nitroxyl species gave the chemical shifts:

δ_H(500 MHz; CD_2Cl_2) 1.72 (6 H, s, C*H*$_3$), 1.82 (6 H, s, C*H*$_3$), 7.02 (1 H, s, CC*H*$_{vin}$C), 7.27 (2 H, d, *J* 8, Ar*H*), 7.39 (2 H, d, *J* 8, Ar*H*), 7.66 (2 H, d, *J* 8, Ar*H*), 7.83 (2 H, d, *J* 8, Ar*H*).

δ_C(500 MHz; CD_2Cl_2) 30.21 (6 C, (*C*H$_3$)$_2$), 31.14 (6 C, (*C*H$_3$)$_2$), 76.26 (1 C, *C*(CH$_3$)$_2$), 78.57 (1 C, *C*(CH$_3$)$_2$), 93.74 (1 C, I*C*(CH)$_2$), 122.38 (2 C, CH$_2$(*C*H)CO), 128.56 (2 C, C(*C*H)(CH)), 129.44 (2 C, CH(*C*H)C), 134.88 (1 C, OC*C*$_{vin}$), 138.48 (2 C, I*C*(CH)), 138.82 (1 C, C*C*(CH)$_2$), 140.03 (1 C, (CH)$_2$*C*C), 144.13 (1 C, C*C*H$_{vin}$C), 150.19 (1 C, CH*C*O), 160.21 (1 C, O*C*O).

m/*z* (APCI$^+$) 463 ([*M* + H]$^+$, 100%); HRMS (APCI$^+$) $C_{21}H_{22}INO_3$ ([*M* + H]$^+$), found 463.0631, requires 463.0639 (– 1.7 ppm).

Found: C, 54.60; H, 4.42; N, 3.15. Calc. for $C_{21}H_{21}INO_3$: C, 54.56; H, 4.58; N, 3.03.

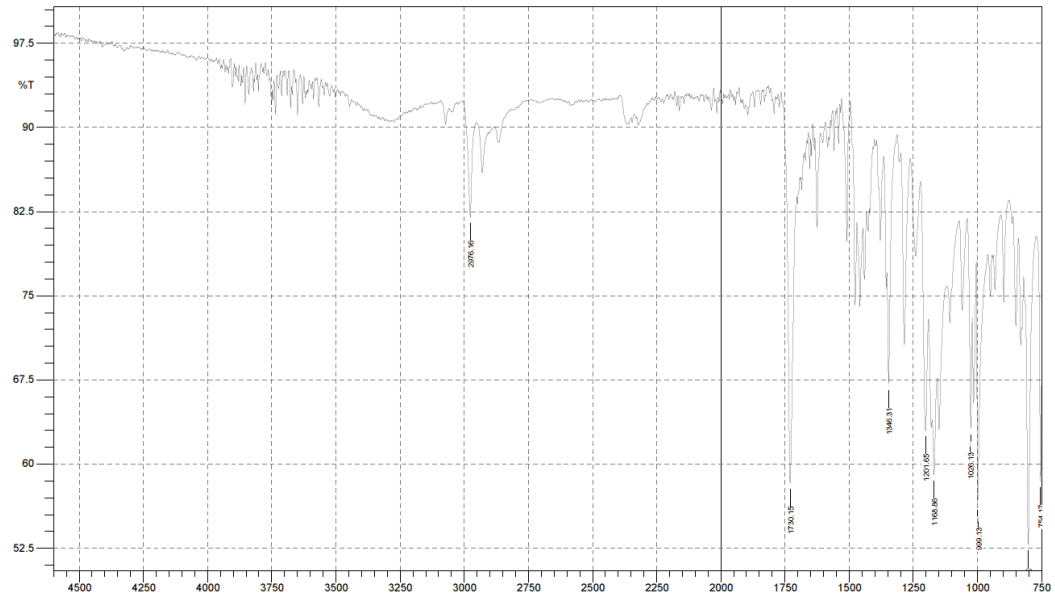

Fig. S1: IR spectrum of compound **1**.

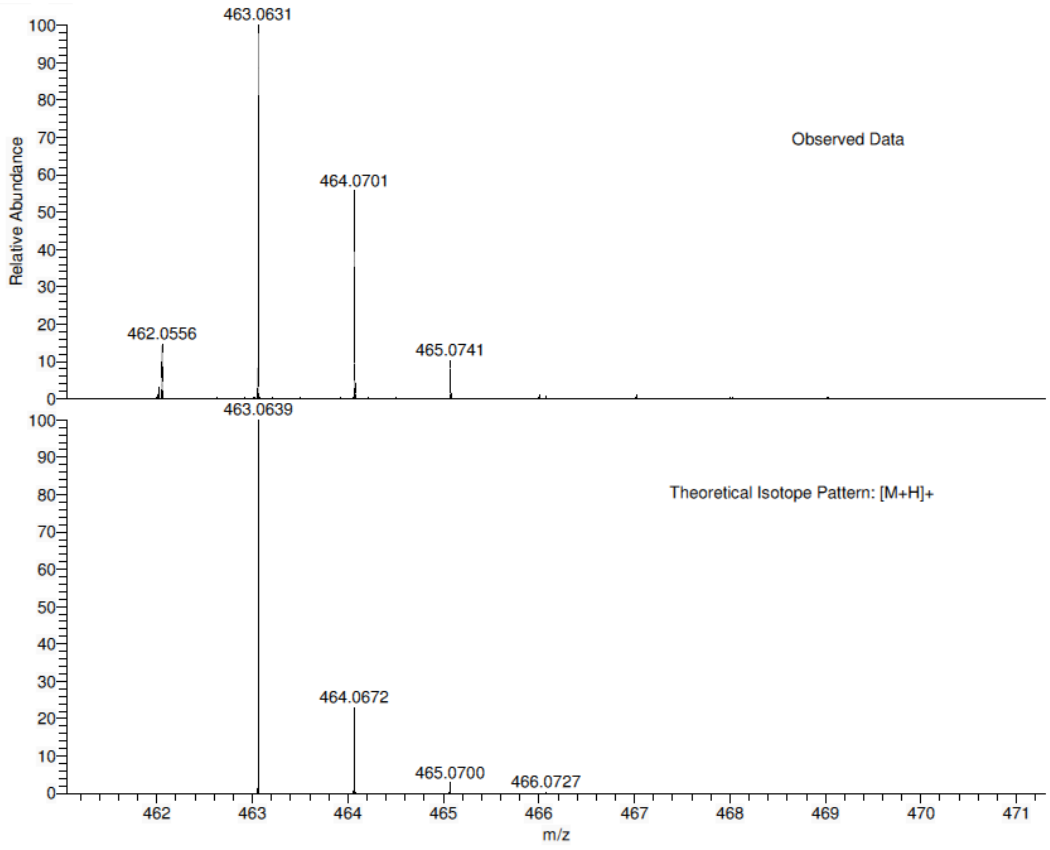

Fig. S2: Mass spectrum of compound **1**.

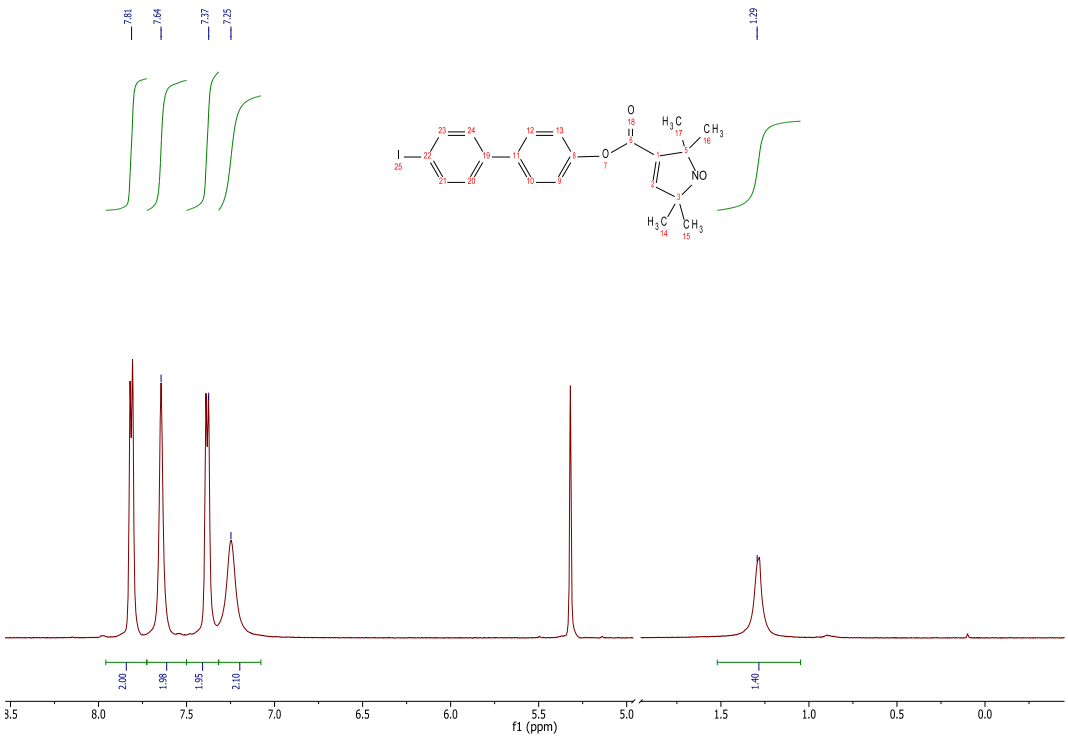

Fig. S3: ^{1}H NMR spectrum of compound **1**.

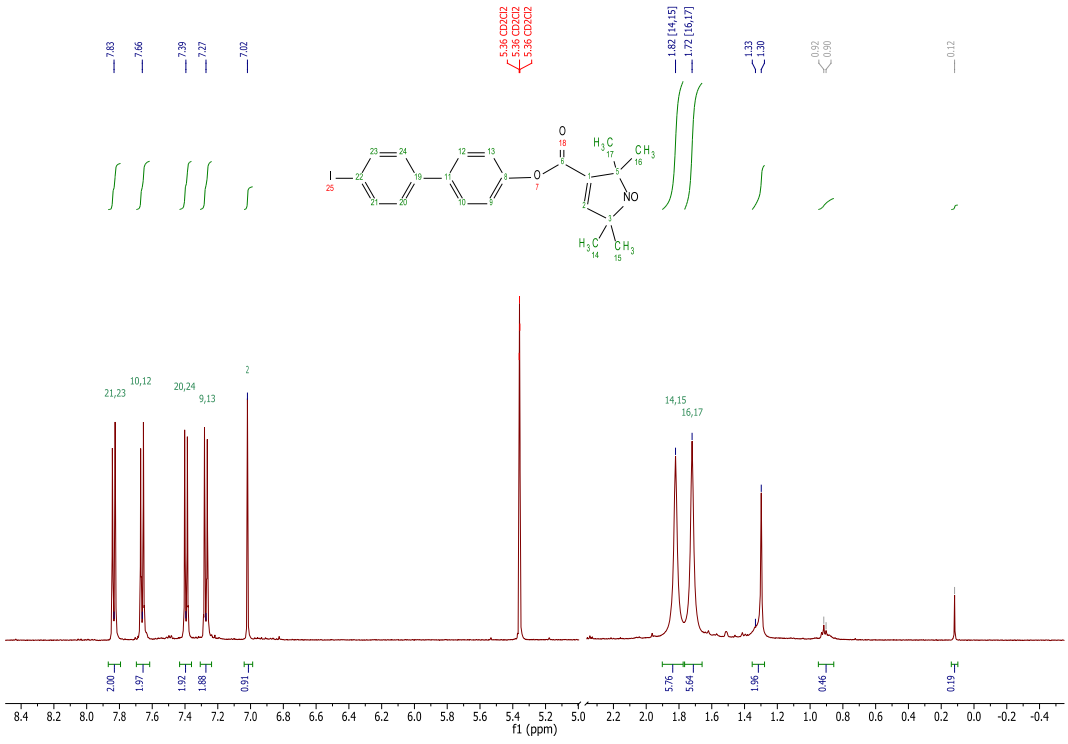

Fig. S4: ^{1}H NMR spectrum of compound **1** after reduction with phenylhydrazine.

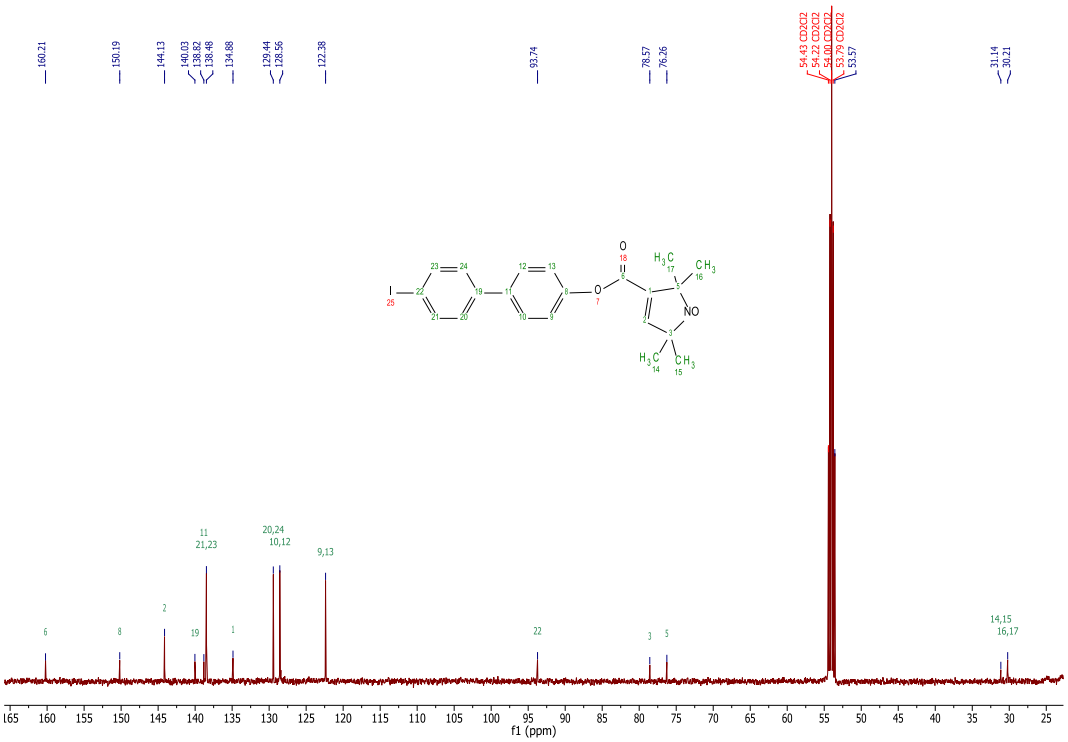

Fig. S5: ^{13}C NMR spectrum of the reduced (by phenylhydrazine) compound **1**.

Crystal structure experimental details of compound **1**:

A. Crystal Data

Empirical Formula	$C_{21}H_{21}INO_3$
Formula Weight	462.31
Crystal Color, Habit	yellow, prism
Crystal Dimensions	0.180 X 0.080 X 0.070 mm
Crystal System	triclinic
Lattice Type	Primitive
Lattice Parameters	a = 11.5839(13) Å
	b = 15.7615(16) Å
	c = 32.762(3) Å
	α = 91.604(3) ^{o}
	β = 91.020(3) ^{o}
	γ = 101.055(3) ^{o}
	V = 5866.7(10) Å^3
Space Group	P-1 (#2)
Z value	12

D_{calc}	1.570 g/cm^3
F_{000}	2772.00
μ(MoKα)	16.577 cm^{-1}

B. Intensity Measurements

Diffractometer	XtaLAB P200
Radiation	MoKα (λ = 0.71075 Å) multi-layer mirror monochromated
Voltage, Current	45kV, 66mA
Temperature	-100.0°C
Detector Aperture	83.8 x 70.0 mm
Data Images	1800 exposures
ω oscillation Range (χ=45.0, ϕ=0.0)	-100.0 - 80.0°
Exposure Rate	5.0 sec./°
Detector Swing Angle	-10.42°
ω oscillation Range (χ=45.0, ϕ=90.0)	-100.0 - 80.0°
Exposure Rate	5.0 sec./°
Detector Swing Angle	-10.42°
ω oscillation Range (χ=45.0, ϕ=180.0)	-100.0 - 80.0°
Exposure Rate	5.0 sec./°
Detector Swing Angle	-10.42°
ω oscillation Range (χ=45.0, ϕ=180.0)	-100.0 - 80.0°
Exposure Rate	5.0 sec./°
Detector Swing Angle	-10.42°
ω oscillation Range (χ=45.0, ϕ=25.0)	-100.0 - 80.0°
Exposure Rate	5.0 sec./°
Detector Swing Angle	-10.42°
Detector Position	45.02 mm
Pixel Size	0.086 mm
$2\theta_{max}$	50.8°
No. of Reflections Measured	Total: 114568 Unique: 21380 (R_{int} = 0.0397)
Corrections	Lorentz-polarization

	Absorption (trans. factors: 0.780 - 0.890)

C. Structure Solution and Refinement

Structure Solution	Direct Methods (SIR2011)
Refinement	Full-matrix least-squares on F^2
Function Minimized	Σ w $(Fo^2 - Fc^2)^2$
Least Squares Weights	$w = 1/ [\sigma^2(Fo^2) + (0.0547 \cdot P)^2 + 2.4315 \cdot P]$ where $P = (Max(Fo^2,0) + 2Fc^2)/3$
$2\theta_{max}$ cutoff	50.8^o
Anomalous Dispersion	All non-hydrogen atoms
No. Observations (All reflections)	21380
No. Variables	1478
Reflection/Parameter Ratio	14.47
Residuals: R1 (I>2.00σ(I))	0.0267
Residuals: R (All reflections)	0.0583
Residuals: wR2 (All reflections)	0.1042
Goodness of Fit Indicator	0.868
Max Shift/Error in Final Cycle	0.002
Maximum peak in Final Diff. Map	0.89 $e^-/Å^3$
Minimum peak in Final Diff. Map	-0.84 $e^-/Å^3$

3. Synthesis and characterisation of compound 2

(4'-[4-{2-(trimethylsilyl)-1-ethynyl}phenyl]-2,2':6',2''-terpyridine)

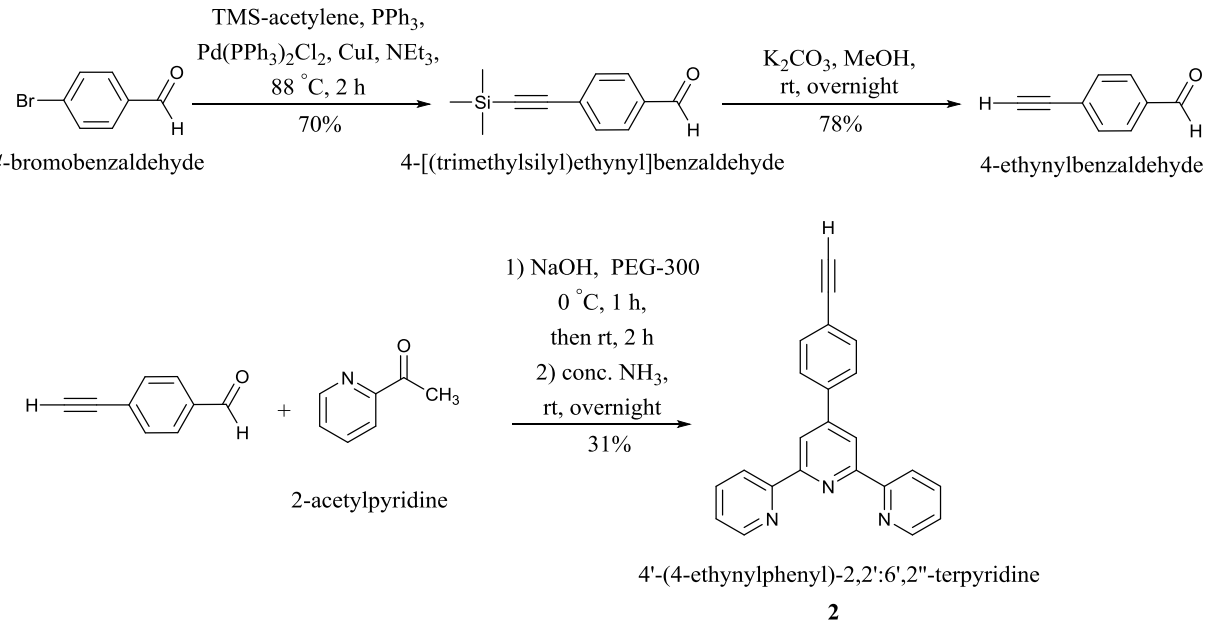

Scheme S2: Synthesis of compound **2**.

The synthesis of 4-[(trimethylsilyl)ethynyl]benzaldehyde was performed as described[2] with minor modifications. Trimethylsilylacetylene (TMS-acetylene) (5.7 mL, 41.0 mmol) and PPh_3 (0.22 g, 0.83 mmol) were dissolved in NEt_3 (15 mL) and degassed by freeze-pump-thaw cycles (× 3). 4-bromobenzaldehyde (5.0 g, 27.0 mmol), $PdCl_2(PPh_3)_2$ (0.24 g, 0.34 mmol) and CuI (0.09 g, 0.49 mmol) were dissolved in NEt_3 (70 mL) and were degassed by freeze-pump-thaw cycles (× 4). The solution of TMS-acetylene was added drop-wise to the solution of the aldehyde over the course of 30 min and the reaction was left stirring at 88 °C for 2 h. After cooling to rt, the solvent was removed *in vacuo* and the black crude product was redissolved in CH_2Cl_2 (150 mL), washed with dist. H_2O (2 × 150 mL) and brine (150 mL). The layers were separated, the organic phase was dried over Na_2SO_4, the solvent was removed *in vacuo* and the crude product was purified by column chromatography on silica (4 × 8 cm, eluent petrol/EtOAc (1/1)) and further sublimated at 45 °C to yield the title compound (3.84 g, 19 mmol, 70%) as white crystalline solid.

Formula: $C_{12}H_{14}OSi$.

δ_H(300 MHz; $CDCl_3$) 0.27 (9 H, s, SiC*H*$_3$), 7.62 (2 H, d, *J* 8, Ar*H*), 7.82 (2 H, d, *J* 8, Ar*H*), 10.00 (1 H, s, C*H*O). The proton chemical shifts are in agreement with published data.[2]

4-[(trimethylsilyl)ethynyl]benzaldehyde (3.83 g, 19 mmol) was treated with 0.1 eq. of K_2CO_3 (0.26 g, 1.9 mmol) in anhydrous MeOH (30 mL) under an atmosphere of N_2 as described[2] with minor modifications. The solution was left stirring overnight at rt, the solvent was removed *in vacuo*, the

orange crude product was redissolved in CH_2Cl_2 (70 mL) and washed with sat. $NaHCO_3$ (3 × 70 mL), dist. H_2O (2 × 70 mL) and brine (70 mL). The layers were separated, the organic phase was dried over $MgSO_4$, the solvent was removed *in vacuo* and the crude product obtained was purified by sublimation at 50 °C yielding 4-ethynylbenzaldehyde (1.96 g, 15.0 mmol, 78%) as white powder.
Formula: C_9H_6O.
δ_H(300 MHz; $CDCl_3$) 3.30 (1 H, s, CC*H*), 7.64 (2 H, d, *J* 8, Ar*H*), 7.85 (2 H, d, *J* 8, Ar*H*), 10.02 (1 H, s, C*H*O). The proton chemical shifts are in agreement with published data.[2]

4'-(4-ethynylphenyl)-2,2':6',2''-terpyridine was prepared according to the procedure described for similar terpyridine based compounds[3] with minor modifications. NaOH pellets (0.91 g, 22.7 mmol) were suspended in PEG-300 (30 mL) and after cooling of the solution to 0 °C, 2-acetylpyridine (4.2 mL, 32.0 mmol) was added. The solution was left stirring at 0 °C for 10 min and the previously synthesised 4-ethynylbenzaldehyde (1.96 g, 15.0 mmol) was added. The mixture was left stirring at 0 °C for 1 h and at rt for further 2 h. During this time the colour of the solution turned from yellow to brown. 35% conc. NH_3 (39 mL, 979 mmol) was added and a red solid formed immediately. The solution was left stirring overnight at rt. The pink precipitate formed was filtered and washed with chilled EtOH (3 × 30 mL) yielding the product (1.55 g, 4.7 mmol, 31%) as a beige powder.
Formula: $C_{23}H_{15}N_3$.
ν_{max}/cm^{-1} 792s, 831s, 1002s, 1165br, 1288s, 1600s (-C≡CH), 1735s. The IR data are in agreement with published data.[4]
δ_H(500 MHz; $CDCl_3$) 3.19 (1 H, s, CC*H*), 7.32 (2 H, ddd, *J* 2.5, 12, Ar*H*), 7.59 – 7.67 (2 H, d, *J* 2, Ar*H*), 7.84 – 7.92 (4 H, m, *J* 2, 8, Ar*H*), 8.67 (2 H, d, *J* 8, Ar*H*), 8.70 – 8.76 (4 H, m, Ar*H*). The proton chemical shifts are in agreement with published data.[4]
m/*z* (NSI$^+$) 334 ([*M* + H]$^+$, 100%); HRMS (NSI$^+$) $C_{23}H_{16}N_3$ ([*M* + H]$^+$), found 334.1333, requires 334.1339 (+ 1.0 ppm).

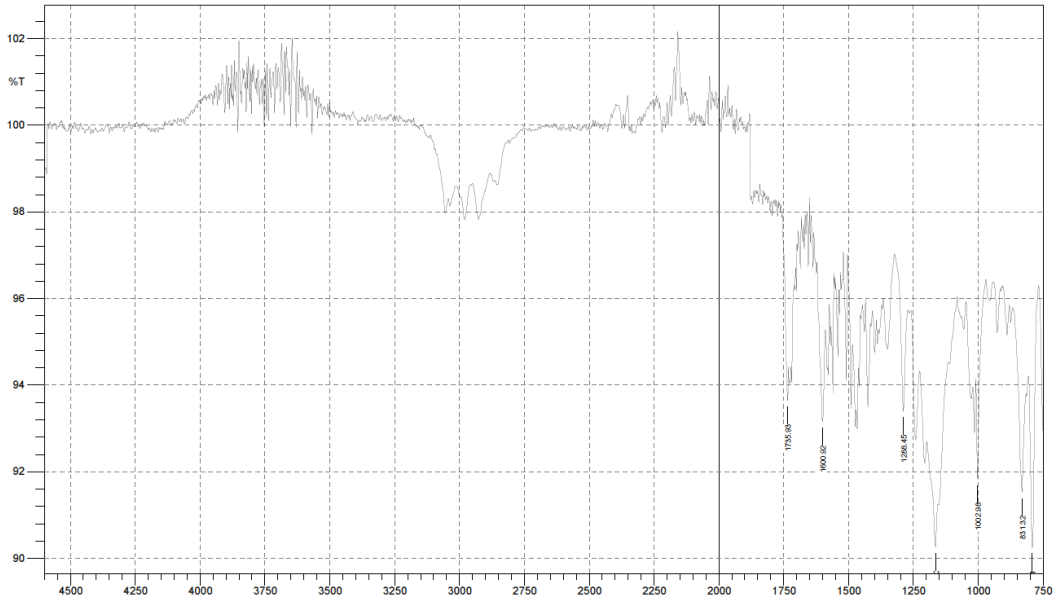

Fig. S6: IR spectrum of compound **2**.

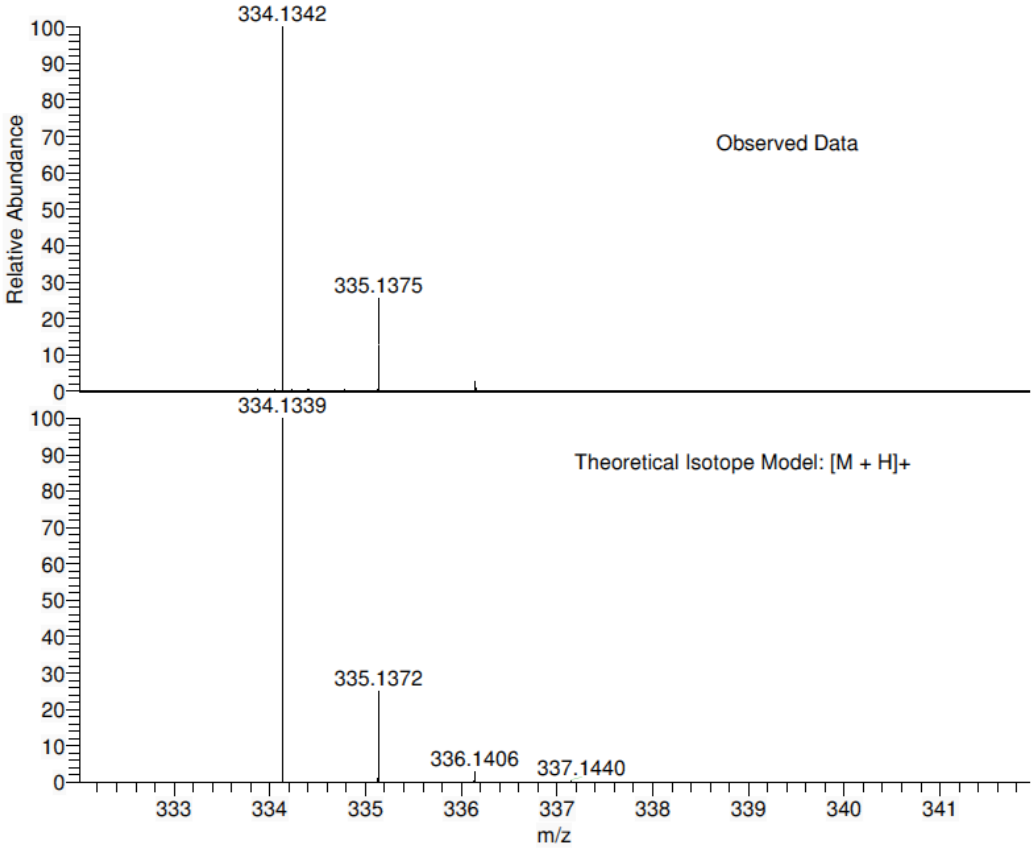

Fig. S7: Mass spectrum of compound **2**.

4. Synthesis and characterisation of compound 3

(4'-((4-([2,2':6',2''-terpyridin]-4'-yl)phenyl)ethynyl)-[1,1'-biphenyl]-4-yl-1-oxyl-2,2,5,5-tetramethyl-2,5-dihydro-1*H*-pyrrole-3-carboxylate)

A solution of 4'-iodo-[1,1'-biphenyl]-4-yl-1-oxyl-2,2,5,5-tetramethyl-2,5-dihydro-1*H*-pyrrole-3-carboxylate **1** (0.23 g, 0.5 mmol) and $PdCl_2(PPh_3)_2$ (0.06 g, 0.08 mmol) in NEt_3 (80 mL) and anhydrous DMF (20 mL) were degassed with freeze-pump-thaw cycles (× 4). 4'-[4-{2-(trimethylsilyl)-1-ethynyl}phenyl]-2,2':6',2''-terpyridine **2** (0.21 g, 0.63 mmol) and PPh_3 (0.06 g, 0.23 mmol) in NEt_3 (20 mL) and anhydrous DMF (5 mL) were degassed with freeze-pump-thaw cycles (× 4). CuI (0.06 g, 0.31 mmol) was added to the first solution followed by drop-wise addition of the first solution to the second over the course of 20 min. The resulting orange solution was left stirring overnight at rt and then heated to 60 °C for 2 h. After cooling of the solution to rt the solvents were removed *in vacuo*, the solid was redissolved in CH_2Cl_2 (100 mL) and washed with H_2O (4 × 100 mL) and brine (4 × 100 mL). The phases were separated, the organic phase was dried over Na_2SO_4 and the solvent was removed *in vacuo*. The crude product was purified by column chromatography on alumina (2 × 9 cm, 4% H_2O) using CH_2Cl_2/MeOH (9.7/0.3)) as eluent. The oily product was taken up in CH_2Cl_2 and addition of hexane led to precipitation of the title compound, which was isolated as a beige powder. The synthesis was repeated multiple times with varying yields (18-89%). Single crystals suitable for X-ray were obtained by layering a chloroform solution of **3** with hexane.

Formula: $C_{44}H_{35}N_4O_3$.

m.p. 188 °C.

ν_{max}/cm^{-1} 734s, 790s, 837s, 1002s, 1166s, 1286s, 1346s, 1386s, 1465s, 1508s, 1583s, 1735s (C=O).

δ_H(400 MHz; CD_2Cl_2) 7.37 (1 H, ddd, *J* 1, 2.7, 12.3, Ar*H*), 7.62 – 7.79 (6 H, m, *J* 8.7, 32, Ar*H*), 7.85 – 7.96 (3 H, m, *J* 8, 2, 2, Ar*H*), 8.64 – 8.74 (3 H, m, *J* 4, 8, Ar*H*), 8.78 (1 H, s, Ar*H*).

Reduction of the nitroxyl radical by phenylhydrazine led to decomposition of the compound.

m/*z* (NSI$^+$) 668 ([*M* + H]$^+$, 100%); HRMS (NSI$^+$) $C_{44}H_{36}N_4O_3$ ([*M* + H]$^+$), found 668.2773, requires 668.2782 (– 1.3 ppm).

Found: C, 78.84; H, 5.35; N, 8.28. Calc. for $C_{44}H_{35}N_4O_3$: C, 79.14; H, 5.28; N, 8.39.

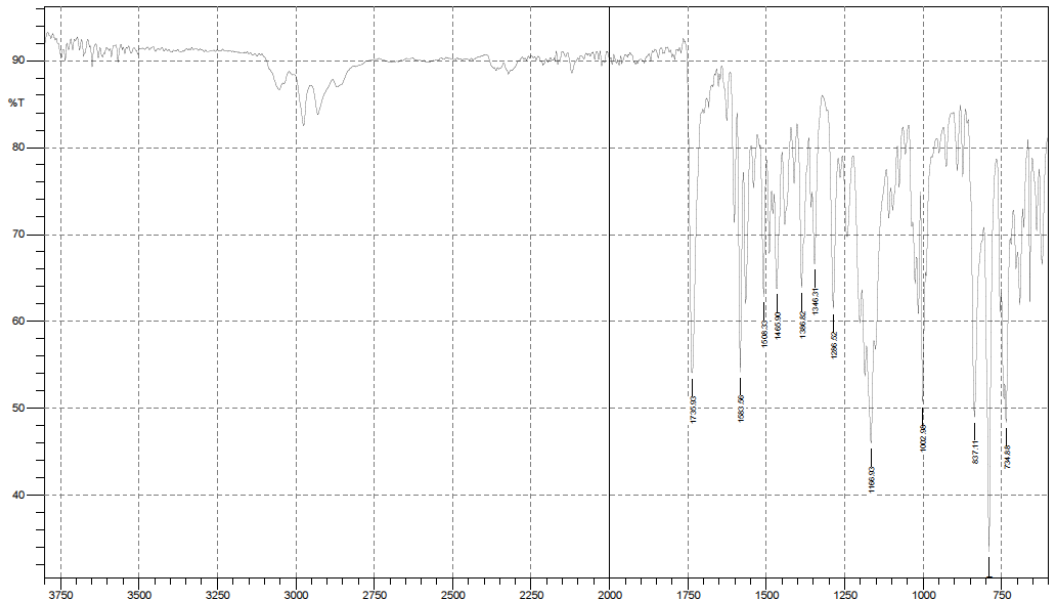

Fig. S8: IR spectrum of compound **3**.

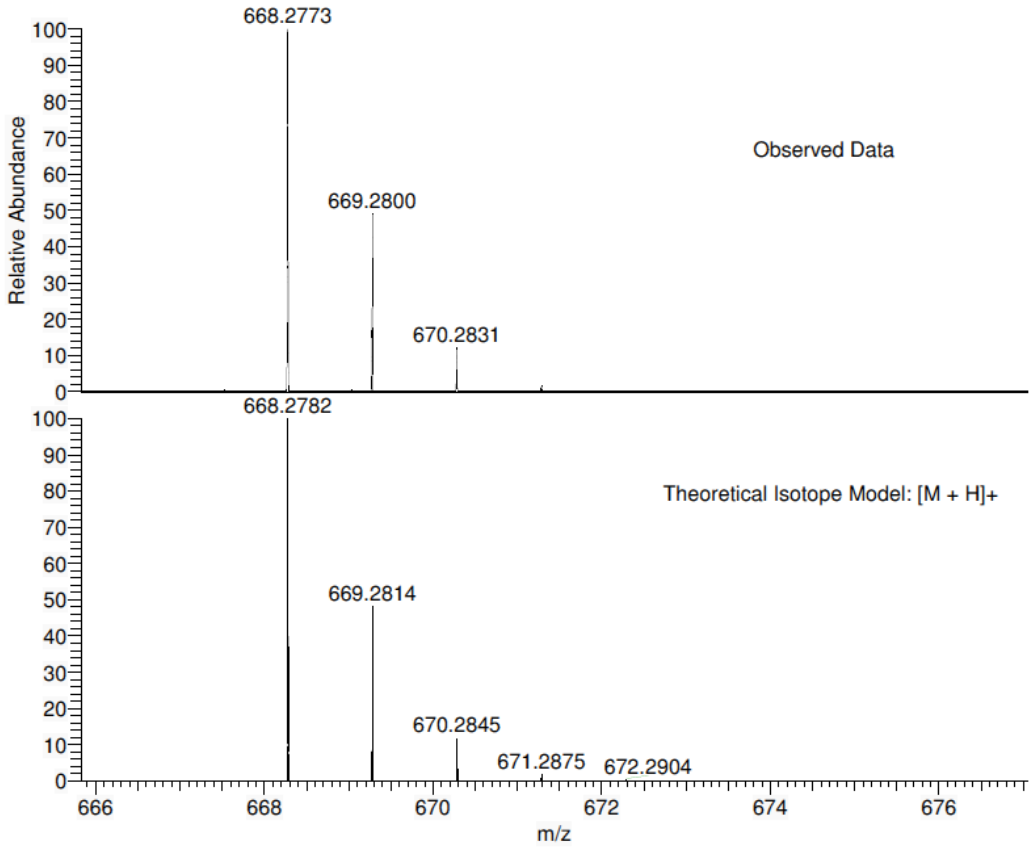

Fig. S9: Mass spectrum of compound **3**.

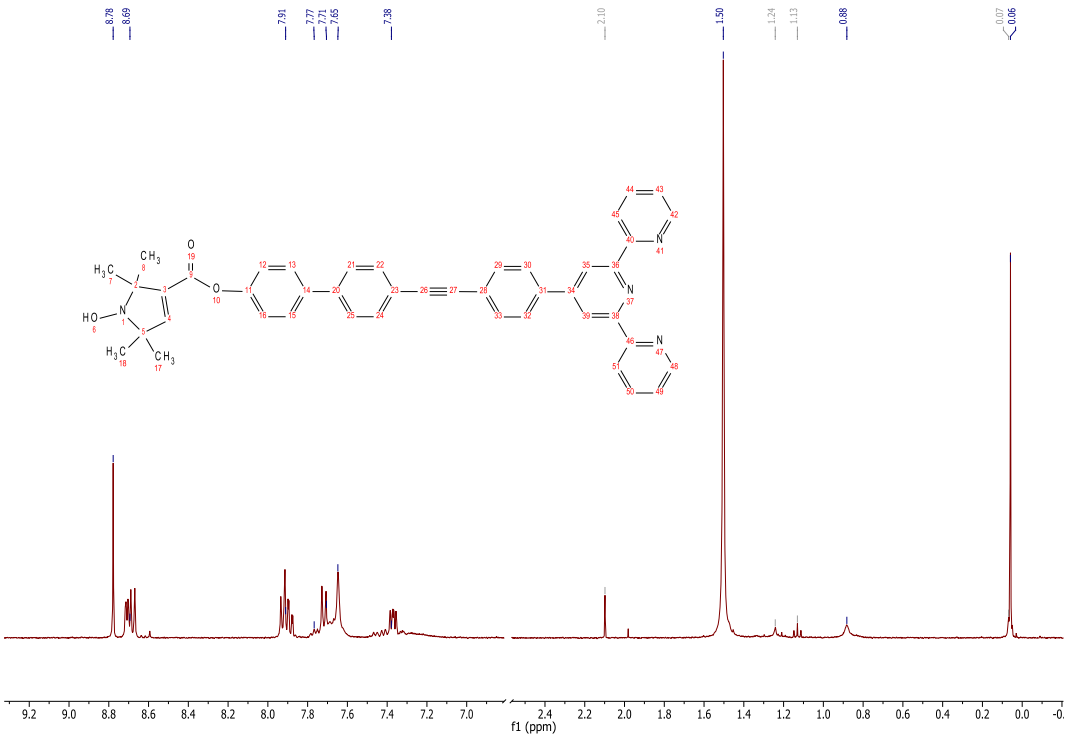

Fig. S10: ^{1}H NMR spectrum of compound **3**.

Crystal structure experimental details of compound **3**:

A. Crystal Data

Empirical Formula	$C_{44.5}H_{36}ClN_4O_3$
Formula Weight	710.25
Crystal Color, Habit	colorless, prism
Crystal Dimensions	0.100 X 0.020 X 0.020 mm
Crystal System	tetragonal
Lattice Type	Primitive
Lattice Parameters	a = 36.726(11) Å
	c = 5.6924(19) Å
	V = 7678(4) Å^3
Space Group	$P4_2/n$ (#86)
Z value	8
D_{calc}	1.229 g/cm^3
F_{000}	2976.00
μ(CuKα)	12.373 cm^{-1}

B. Intensity Measurements

Diffractometer	XtaLAB P200
Radiation	CuKα (λ = 1.54187 Å) multi-layer mirror monochromated
Voltage, Current	40kV, 30mA
Temperature	-148.0°C
Detector Aperture	83.8 x 70.0 mm
Data Images	3112 exposures
Pixel Size	0.172 mm
$2\theta_{max}$	136.4°
No. of Reflections Measured	Total: 59425 Unique: 6909 (R_{int} = 0.1388)
Corrections	Lorentz-polarization Absorption (trans. factors: 0.440 - 0.976)

C. Structure Solution and Refinement

Structure Solution	Direct Methods (SIR2011)
Refinement	Full-matrix least-squares on F^2
Function Minimized	Σ w $(Fo^2 - Fc^2)^2$
Least Squares Weights	$w = 1/ [\sigma^2(Fo^2) + (0.2000 \cdot P)^2$ $+ 0.0000 \cdot P]$ where $P = (Max(Fo^2,0) + 2Fc^2)/3$
$2\theta_{max}$ cutoff	136.5°
Anomalous Dispersion	All non-hydrogen atoms
No. Observations (All reflections)	6909
No. Variables	527
Reflection/Parameter Ratio	13.11
Residuals: R1 (I>2.00σ(I))	0.1365
Residuals: R (All reflections)	0.1648
Residuals: wR2 (All reflections)	0.4042
Goodness of Fit Indicator	1.612
Max Shift/Error in Final Cycle	0.084
Maximum peak in Final Diff. Map	1.65 $e^-/Å^3$
Minimum peak in Final Diff. Map	-0.67 $e^-/Å^3$

5. Complexation of Zn(II) and 3 – Formation of the bis-complex

($Zn(tpyNO)_2^{2+}$)

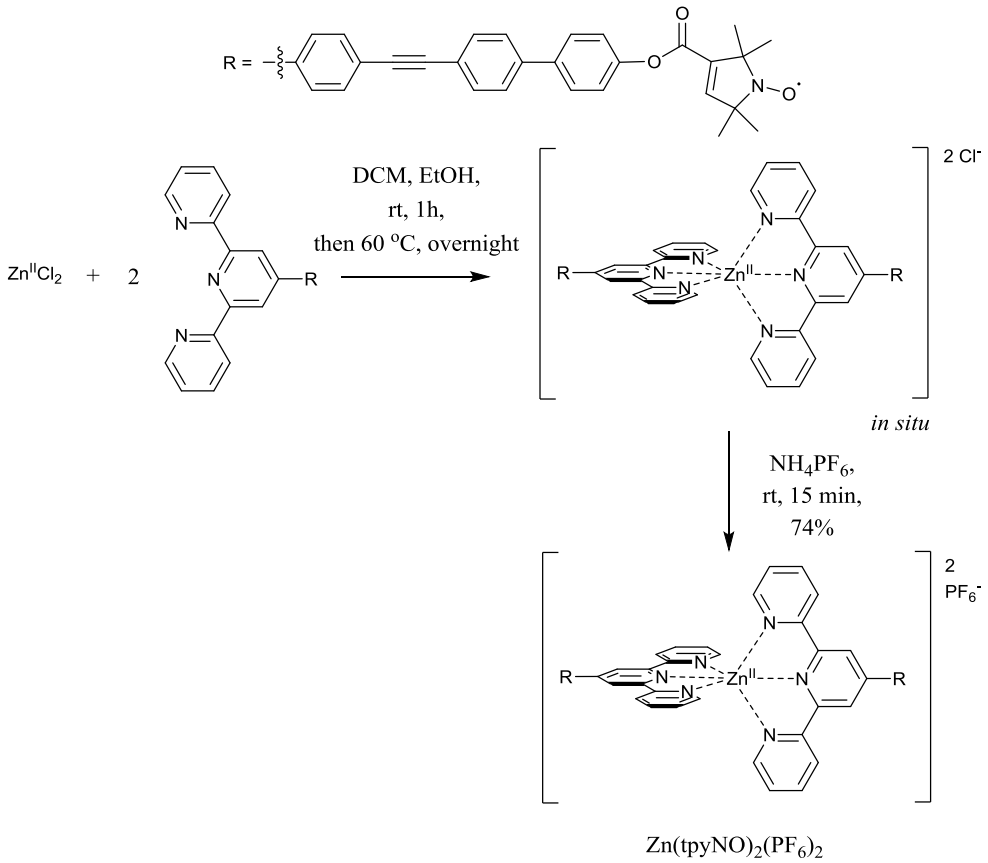

Scheme S3: Synthesis of complex $Zn(tpyNO)_2(PF_6)_2$.

Zinc(II) chloride (0.003 g, 0.02 mmol) was dissolved in EtOH (3 mL) and ligand **3** (0.027 g, 0.04 mmol) was dissolved in CH_2Cl_2 (3 mL). After stirring of both solutions at rt for 15 min, the Zn(II) chloride solution was added to the ligand solution and the colour of the latter turned pale yellow. The reaction mixture was left stirring at rt for 1 h, then at 60 °C overnight. After cooling to rt excess NH_4PF_6 (0.04 g, 0.25 mmol) was added. A precipitate started forming immediately and the reaction mixture was left stirring at rt for overnight. The product (0.025 g, 0.015 mmol, 74%) was isolated with filtration as pale yellow powder. An alternative preparation without overnight refluxing ("mix-and-measure") used for the titration experiment is detailed in the next chapter. For EPR sample preparation, a ten-fold excess of $NaBPh_4$ was added for increased solubility.

Formula: $C_{88}H_{70}N_8O_6ZnF_{12}P_2$.

m.p. >300 °C.

ν_{max}/cm^{-1} 790s, 830s, 1002s, 1166s, 1288s, 1427s, 1473s, 1600s, 1732s (C=O).

m/*z* (MALDI - DCTB) 1400 ($[M - 2PF_6]^+$, 100%).

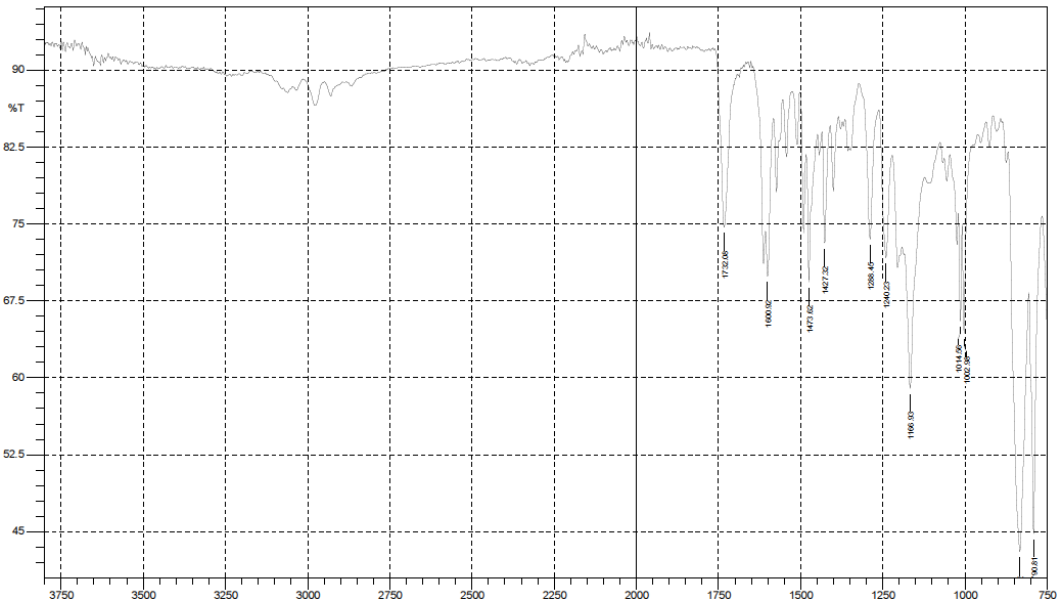

Fig. S11: IR spectrum of $Zn(tpyNO)_2(PF_6)_2$.

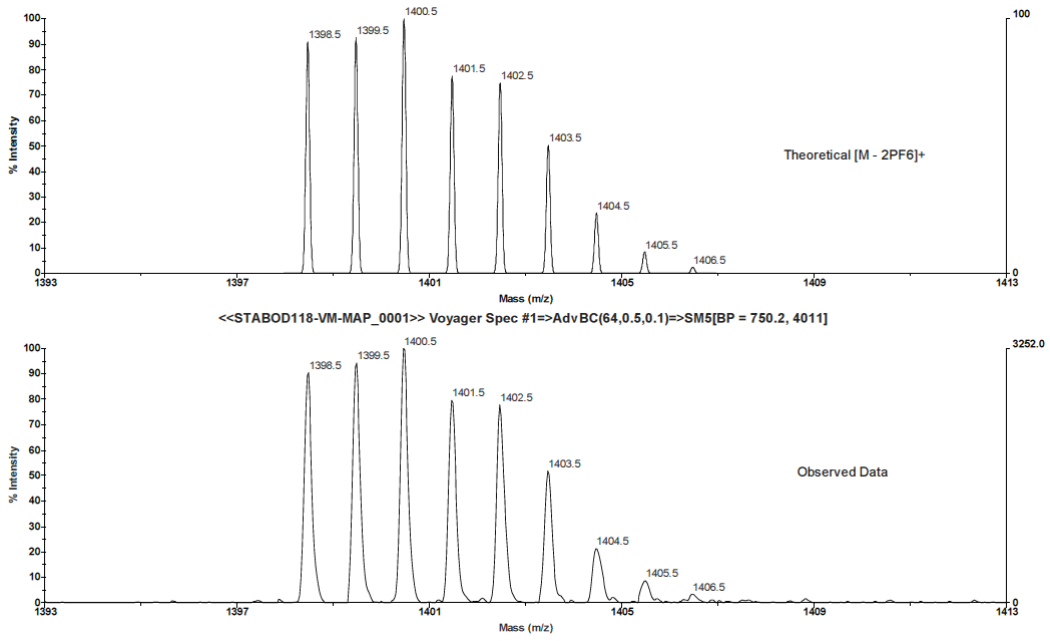

Fig. S12: Mass spectrum of $Zn(tpyNO)_2^{2+}$ revealing the formation of the bis-complex.

6. Optimisation of complex and sample preparation for EPR measurements

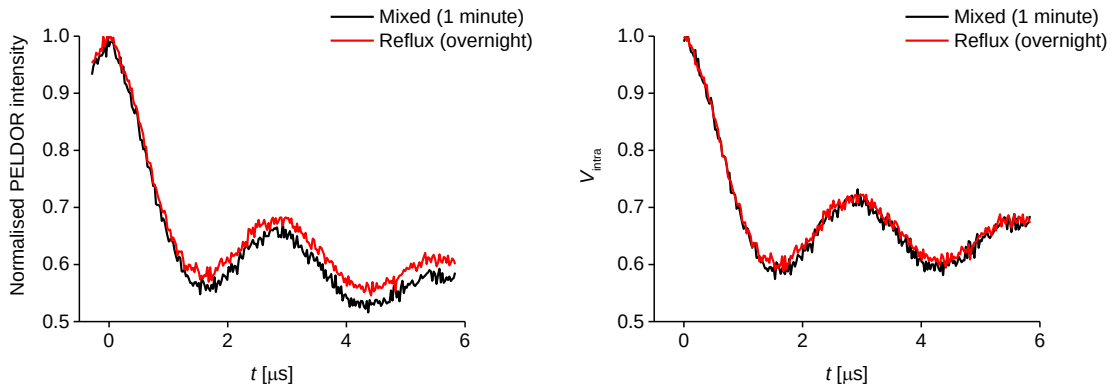

Fig. S13: Raw (*left*) and background-corrected (*right*) time traces comparing preparation methods for the Zn(II)/tpyNO complex used for titration.

Two preparation methods were tested: the reaction batch was either refluxed overnight and precipitated with hexafluorophosphate or just mixed for 1 minute by pipetting up and down before drying under vacuum. After background-correction both preparation methods gave virtually the same modulation depth. Thus, the titration samples were prepared according to the "mix-and-measure" method.

A total of 11 samples was prepared for the EPR titration experiment. The concentration of the ligand was kept constant at 100 µM final concentration, while the Zn(II)/ligand molar ratio was varied from 0.0 to 1.0 in 0.1 steps. The final volume of each reaction batch was kept constant at 100 µl (50 µl EtOH/50 µl DCM). Upon mixing the constituents by pipetting up and down for 1 minute, the solution was dried under vacuum. $NaBPh_4$ was added to the dried sample in ~10-fold excess before resolubilisation in 80 µl DMSO-d_6. 20 µl of a 1:1 D_2O:ethylene glycol mixture was added slowly to avoid any precipitation. The solution was briefly mixed by pipetting up and down, filled into a 4 mm EPR quartz tube (Wilmad) and immediately frozen in liquid nitrogen. A second titration series consisting of an independent set of 11 samples was prepared as described above.

7. EPR instrumentation and collection of PELDOR data

PELDOR data were recorded on an ELEXSYS E580 pulsed X-band EPR spectrometer (~9 GHz) including the second frequency option (E580-400U) from Bruker. Pulses were amplified by a 1 kW travelling wave tube (TWT) amplifier (Applied Systems Engineering). An MD5 dielectric ring resonator with standard flex line probe head was used. The established 4-pulse DEER pulse sequence $\pi/2(\nu_A)$-τ_1-$\pi(\nu_A)$-τ_1+t-$\pi(\nu_B)$-(τ_2–t)-$\pi(\nu_A)$-τ_2-echo was employed for all PELDOR experiments.[5] With the following exceptions of timings and pump pulse length chosen settings and optimisation procedures were as previously described.[6] For all samples, the pump pulse was set to 18 ns, τ_1 to 380 ns, τ_2 to 3.55 μs to measure more than one full modulation (6 μs in addition for samples with ratios 0.1, 0.5, and 1) and the shot repetition time to 3 ms, averaging the data for ~35 min per sample (5 scans on average; longer averaging time for the 6 μs time window). Samples of the first titration series were measured three times, independently, to estimate the measurement error from the standard deviation, while the second titration series served as an indication of the deviations between sample preparations.

8. EPR titration series – additional PELDOR data

Given are the raw PELDOR data (Fig. S14) and corresponding distance distributions (Fig. S15) from the titration experiment (first measurement series). In addition to the main peak some artefacts potentially resulting from a worse signal-to-noise ratio could be observed in low-ratio samples (0.1 - 0.3) only. Even when using a longer time window (Fig. S16; 6 μs instead of 3.55 μs) the PELDOR experiment at ratio 0.1 showed some artefacts.

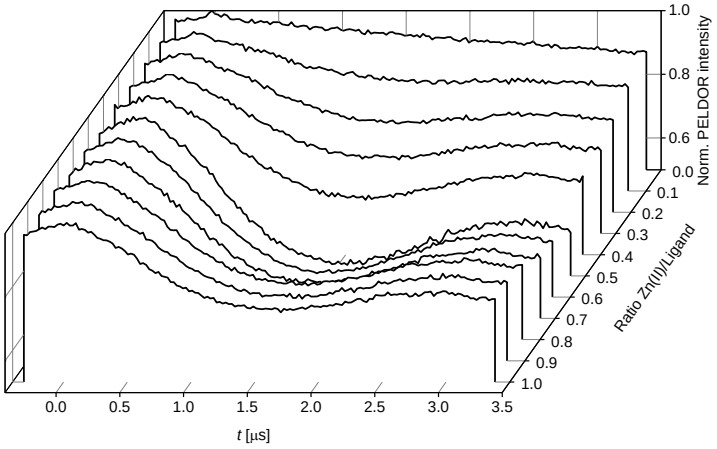

Fig. S14: Waterfall plot of the 11 raw PELDOR traces (no background correction) from the titration experiment.

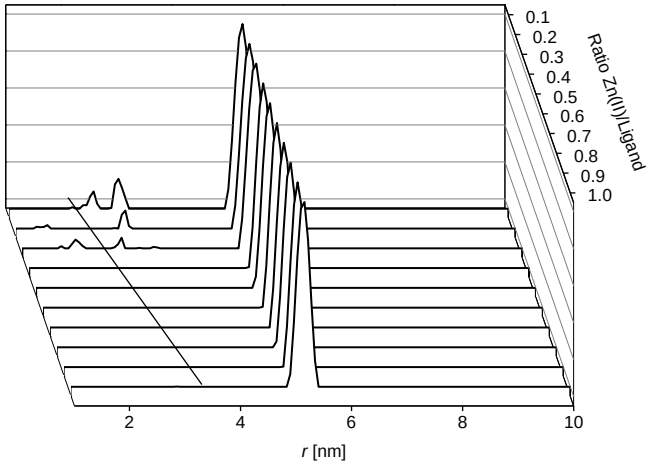

Fig. S15: Derived distance distributions from the titration series as obtained by Tikhonov regularisation.

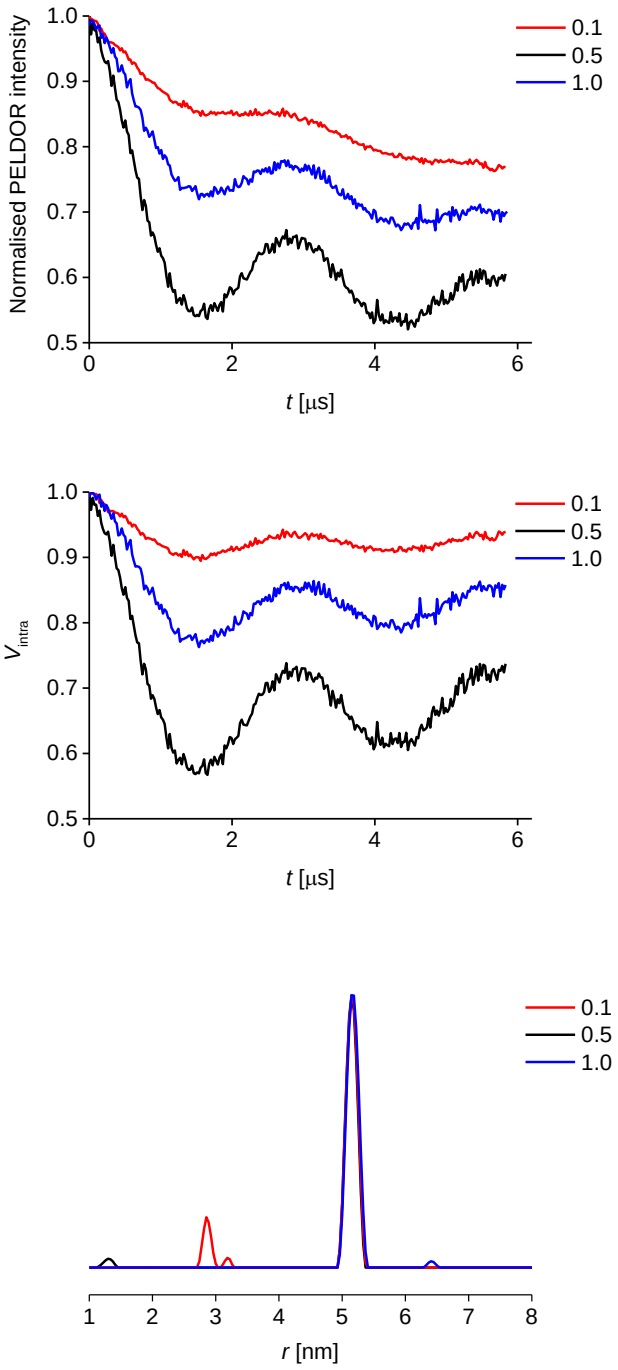

Fig. S16: Raw (*top*) and background-corrected (*middle*; using the monomer density value as described in the main text) time traces with 6 µs time window. *Bottom* Derived distance distributions. Note the artefact at ~2.9 nm for ratio 0.1 only.

9. Models for Zn(II)/tpy bis-complex formation

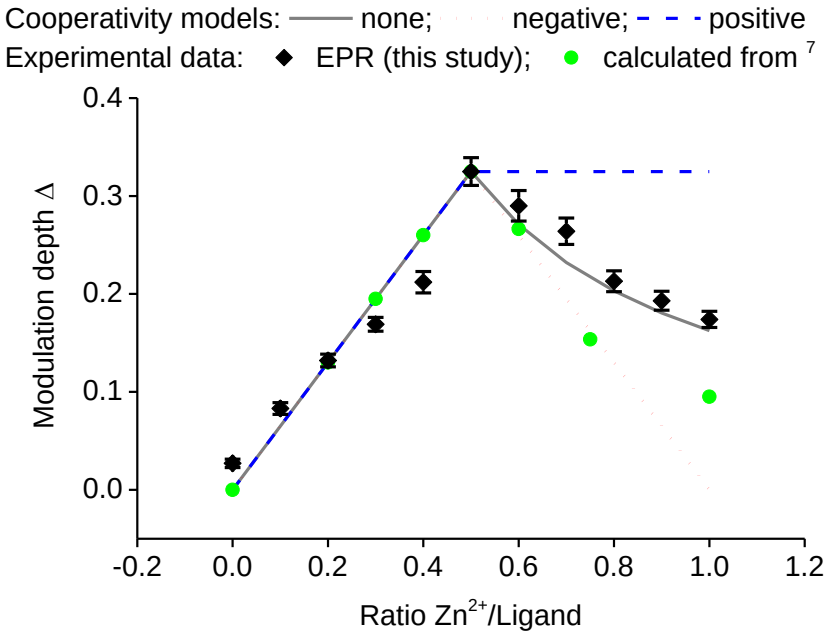

Fig. S17: Experimental modulation depths Δ (EPR – this study; re-calculated from NMR data[7]) and respective cooperativity models, all based on our experimentally obtained maximum modulation depth of 0.33 at a ratio of 0.5 (first measurement series) , and the corresponding error of fit (root mean square deviation).

10. Effect of background correction and sample preparation

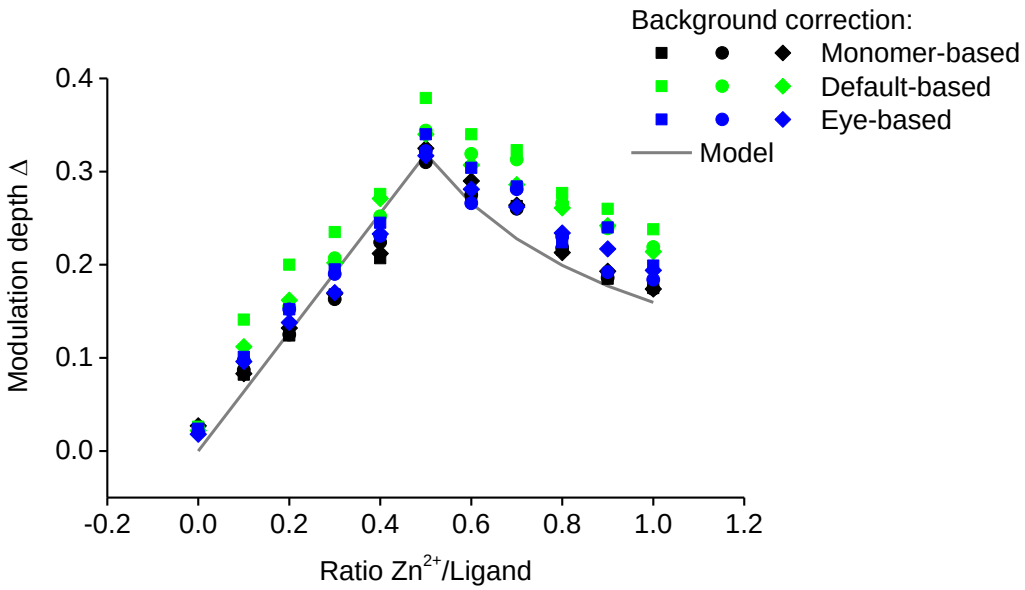

Fig. S18: Effect of different background correction strategies using three independent measurements per sample. Results obtained with the 'true' background correction based on the decay constant of the monomer are shown in black. The (trained) eye-based background correction (blue) shows slightly larger differences compared to the monomer-informed correction. The background correction based on the DeerAnalysis fit option (green) shows the largest deviations, consistently leading to a larger modulation depth.

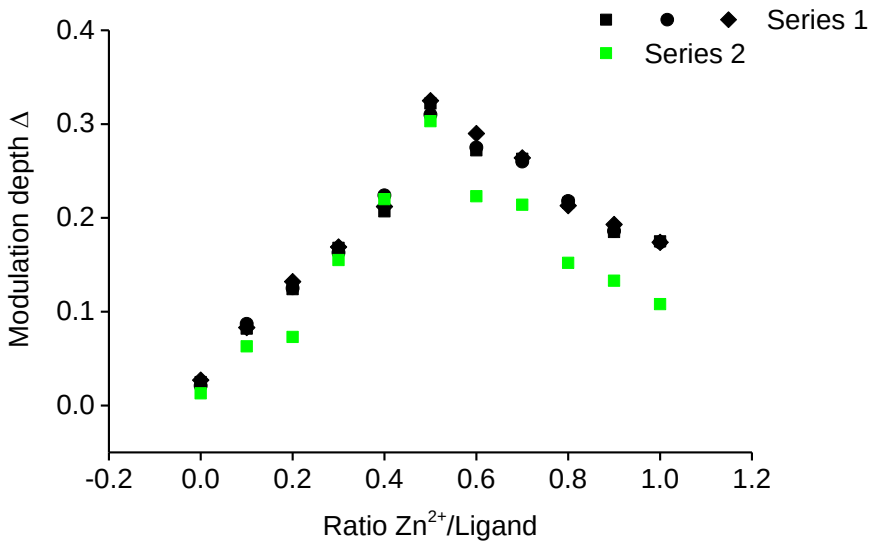

Fig. S19: Effect of different sample preparations on the observed titration curve. A second titration series gave a modulation depth of 0.30 at ratio 0.5, instead of the previously observed mean modulation depth of 0.32 for the first series (independent set of 3 measurements per sample). The shape of the titration curve is well reproducible though. We conclude that in the present case the error introduced by individual sample preparation is larger than the PELDOR measurement error within the same series (compare to Fig. S18).

Table S1: Comparison of experimentally obtained standard deviation (SD; set of 3 independent measurements per sample in series 1), error of fit (RMSD; first measurement round in series 1), and the difference in Δ between titration series 1 and 2.

Ratio	**SD**	**RMSD**	**$\Delta_1 - \Delta_2$**
0.0	0.003	0.004	0.011
0.1	0.003	0.006	0.021
0.2	0.004	0.007	0.054
0.3	0.003	0.007	0.012
0.4	0.009	0.011	-0.006
0.5	0.008	0.014	0.016
0.6	0.010	0.016	0.056
0.7	0.002	0.013	0.048
0.8	0.003	0.011	0.064
0.9	0.004	0.010	0.055
1.0	0.001	0.008	0.066

11. Determination of dissociation constant and error propagation

While in this study we are investigating a biomimetic model system, recent work from our lab demonstrates that also biological systems can show modulation depths in good agreement with binding constants from other methods.[8] For a non-templated dimerisation system such as a protein dimer, the dissociation constant K_D can in principle be derived from the PELDOR modulation depth and the sample concentration provided a decent signal-to-noise ratio of the PELDOR trace and a reliable background correction.

The fraction of spin labels in dimers x_D can be given as:

$$x_D = \frac{\Delta}{\lambda}$$

and the fraction of spin labels in monomers x_M as:

$$x_M = 1 - \frac{\Delta}{\lambda}.$$

The dissociation constant K_D can be expressed using the concentrations of monomer and dimer as follows:

$$K_D = \frac{[M]^2}{[D]}.$$

Thus, K_D can be expressed as a function of the sample concentration c_S, the experimental modulation depth Δ, and the pump efficiency λ:

$$K_D = \frac{2\, c_S\, \lambda\, (\frac{\Delta}{\lambda}-1)^2}{\Delta}.$$

For an estimation of the error in the determination of K_D from our titration curve, we assumed an error in the sample concentration of 5%, and a λ of 0.33 ± 0.01. For each titration step between ratio 0.0 and ratio 0.4 the experimentally obtained modulation depth and its corresponding error of fit (root mean square deviation) was used (Fig. S20, black line, Table S2). In addition, a second, theoretical set of parameters was analysed, assuming the same sample concentration, but a λ of 0.40 ± 0.02,[6] which may come closer to values obtained for a biological system. The modulation depth was varied from 0.05 to 0.35 in 0.05 steps, with an assumed error in Δ of 0.01 (Fig. S20, red line, Table S2). As expected the K_D will be most reliable when the sample concentration is in the same order of magnitude.

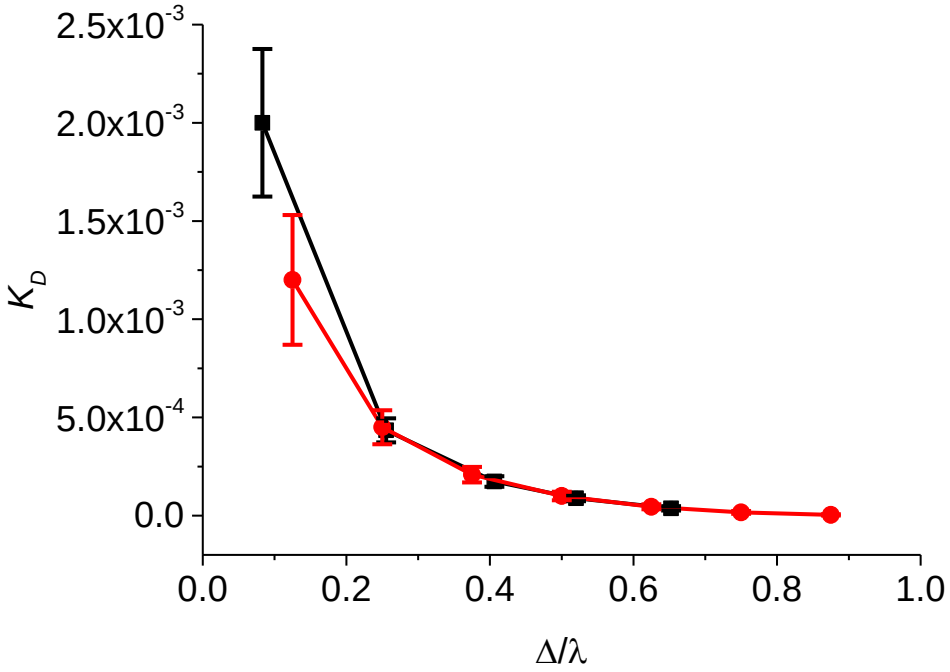

Fig. S20: Reliability of K_D determination. Details are given within the text.

Table S2: K_D determination

Fig. S20 Black Line			**Fig. S20 Red Line**		
Δ/λ	**K_D**	**Error**	**Δ/λ**	**K_D**	**Error**
0.083	2.00×10^{-3}	3.8×10^{-4}	0.125	1.20×10^{-3}	3.3×10^{-4}
0.255	4.34×10^{-4}	6.1×10^{-5}	0.250	4.50×10^{-4}	8.7×10^{-5}
0.406	1.74×10^{-4}	2.7×10^{-5}	0.375	2.08×10^{-4}	4.0×10^{-5}
0.520	8.9×10^{-5}	1.5×10^{-5}	0.500	1.00×10^{-4}	2.2×10^{-5}
0.652	3.7×10^{-5}	1.1×10^{-5}	0.625	4.5×10^{-5}	1.3×10^{-5}
			0.750	1.67×10^{-5}	7.1×10^{-6}
			0.875	3.6×10^{-6}	3.1×10^{-6}

In the above error propagation, the total error of the determination in the dissociation constant was estimated from the individual uncertainties in sample concentration, experimental Δ, and the pump efficiency λ. Assuming that the uncertainty in Δ (σ_Δ) dominates, the uncertainty in the determination of K_D (σ_K) can be simplified to:

$$\sigma_K = \frac{2\ c_S\ (\Delta^2 - \lambda^2)}{\Delta^2\ \lambda} \sigma_\Delta\ .$$

12. References

1 B. E. Bode, J. Plackmeyer, T. F. Prisner and O. Schiemann, *J. Phys. Chem. A*, 2008, **112**, 5064-5073.

2 W. B. Austin, N. Bilow, W. J. Kelleghan and K. S. Y. Lau, *J. Org. Chem.*, 1981, **46**, 2280-2286.

3 A. Winter, A. M. J. van den Berg, R. Hoogenboom, G. Kickelbick and U. S. Schubert, *Synthesis*, 2006, **17**, 2873-2878.

4 V. Grosshenny, F. M. Romero and R. Ziessel, *J. Org. Chem.*, 1997, **62**, 1491-1500.

5 M. Pannier, S. Veit, A. Godt, G. Jeschke and H. W. Spiess, *J. Magn. Reson.*, 2000, **142**, 331-340.

6 B. E. Bode, D. Margraf, J. Plackmeyer, G. Dürner, T. F. Prisner and O. Schiemann, *J. Am. Chem. Soc.*, 2007, **129**, 6736-6745.

7 R. Dobrawa, P. Ballester, C. R. Saha-Moller and F. Wurthner, in *Metal-containing and metallosupramolecular polymers and materials*, eds. U. S. Schubert, G. R. Newkome and I. Manners, American Chemical Society, 2006, vol. 928, pp. 43-62.

8 P. S. Kerry, H. L. Turkington, K. Ackermann, S. A. Jameison and B. E. Bode, *J. Phys. Chem. B*, 2014, **118**, 10882-10888.